

# Influence of Steam Dilution on the Combustion of Natural Gas and Hydrogen in Premixed and Rich-Quench-Lean Combustors

Sebastian Göke<sup>a,1,\*</sup>, Marc Füre<sup>b,2</sup>, Gilles Bourque<sup>b,2</sup>, Bernhard Bobusch<sup>a,1</sup>, Katharina Göckeler<sup>a,1</sup>, Oliver Krüger<sup>a,1</sup>, Sebastian Schimek<sup>a,1</sup>, Steffen Terhaar<sup>a,1</sup>, Christian Oliver Paschereit<sup>a,3</sup>

<sup>a</sup>Chair of Fluid Dynamics, – Hermann-Föttinger-Institute –, Technische Universität Berlin, Germany

<sup>b</sup>Rolls-Royce Canada, Montreal, Canada

---

## Abstract

The combustion of different natural gas - hydrogen mixtures at dry and steam-diluted conditions is investigated for a Rich-Quench-Lean (RQL) and for a premixed combustor. Atmospheric experiments are conducted over a wide range of equivalence ratios and degrees of steam dilution up to a steam-to-air mass ratio of 30%. Emission formation, flame shape and position, and flame stability are measured in combustion tests. An investigation of the influence of steam on the NO<sub>x</sub> formation is conducted using reactor networks.

Steam effectively inhibits the formation of NO<sub>x</sub> emissions in both combustion systems. For wet conditions, NO<sub>x</sub> emissions below 10 ppm are achieved for operation on natural gas as well as hydrogen up to high equivalence ratios and temperatures. Increasing the hydrogen content leads to increasing NO<sub>x</sub> emissions for dry conditions, whereas at wet conditions, NO<sub>x</sub> is lower for hydrogen-rich fuels. The numerical analysis reveals that in both combustion systems, the thermal, the N<sub>2</sub>O, and the NNH pathways are significantly constrained at wet conditions. The prompt NO<sub>x</sub> can be increased due to higher CH radical concentrations for the natural gas flame. CO emissions remain low up to moderate degrees of steam dilution. For a steam content of 20%, the RQL combustor shows increasing CO emissions for low equivalence ratios, whereas they remain low for the premixed combustor.

Steam dilution is very effective for NO<sub>x</sub> reduction in natural gas and in hydrogen flames. Additionally, it lowers the reactivity of hydrogen and already a relatively low steam content prevents flashback. The combination of steam injection and hydrogen combustion provides an efficient and clean combustion mode.

---

## 1. Introduction

Humidified gas turbines operating at ultra-wet conditions offer a significant increase in efficiency compared to the dry gas turbine cycle. In single-cycle application, ultra-wet gas turbines reach efficiencies comparable to state of the art combined-cycle power plants with up to 55% - 60%[1], but with much lower installation costs and emission levels. In contrast to the complex combined-cycle plants, ultra-wet gas turbines have a substantially smaller footprint. Depending on the cycle configuration, short start-up times and excellent load control capabilities can be achieved. Furthermore, the high steam content allows for low-NO<sub>x</sub>, near-stoichiometric combustor operation and thus enables post-combustion CO<sub>2</sub> capture at low cost, since the concentration of CO<sub>2</sub> reaches the highest possible value for air breathing gas turbines after condensation of the steam. Moreover, the reactivity of hydrogen is significantly reduced by the steam injection, thereby enabling clean and efficient operation using hydrogen-rich fuels from biomass or coal gasification, and pure hydrogen.

---

\*Corresponding author

Email address: [sebastian.goeke@tu-berlin.de](mailto:sebastian.goeke@tu-berlin.de) (Sebastian Göke)

<sup>1</sup>PhD student, Chair of Fluid Dynamics

<sup>2</sup>Combustion specialist

<sup>3</sup>Professor, Chair of Fluid Dynamics

A number of studies have investigated the influence of steam on the combustion process. It was shown that steam dilution can have a strong influence on the combustion process and affects the concentrations of the chain branching species O, OH, and H [2]. At wet conditions, the autoignition delay times are increased [3], and the laminar burning velocities are reduced [4, 5].

Concerning NO<sub>x</sub> emissions, steam injection affects the emission formation in two ways [6]. It reduces the flame temperature, and therewith restrains the thermal NO<sub>x</sub> formation pathway which contributes most to overall NO<sub>x</sub> emissions at temperatures above approximately 1800 K. The steam additionally has a chemical influence. The increased steam concentration, together with the reduced concentrations of oxygen and nitrogen, affect the reaction kinetics by changing the concentration of active species which are involved in the NO<sub>x</sub> formation. The influence of steam dilution on the different formation pathways, however, is reported differently in literature. For a natural gas diffusion flame, Zhao et al. [7] found that steam leads to higher emissions through the thermal pathway, but is constrained as a whole by significantly lower prompt NO<sub>x</sub>. Bhargava et al. [8] assessed a premixed combustor and concluded that steam reduces NO<sub>x</sub> formation through all assessed pathways. This is in contrast to a recent study for premixed flames [9], which found that the prompt pathway is possibly even slightly increased at wet conditions, while the other pathways are significantly reduced due to lower oxygen atom concentrations, leading to reduced overall NO<sub>x</sub> emissions.

The influence of steam injection on CO emissions seems to depend strongly on the combustor configuration and the operating conditions. While some authors state that steam injection increases CO emissions [10], others found that CO is not affected by steam [11], or even slightly reduced [12, 13].

In the current study, the influence of steam dilution on the combustion of natural gas and hydrogen is investigated for a Rich-Quench-Lean (RQL) and for a premixed combustor. Combustion experiments are conducted over a wide range of equivalence ratios from near-stoichiometric conditions to lean blowout, and steam content in the air between 0% and 30% by mass. The influence of steam on NO<sub>x</sub> and CO emissions formation, flame shape, and flame stability is investigated. Two reactor networks are designed and validated with the experimental results. They are used to gain further insight into the emission formation for natural gas and hydrogen for the different combustion approaches.

## 2. Experiments

### 2.1. Combustion Test Rig

The experiments with the premixed and the RQL combustors are conducted on a modular combustion test rig at TU Berlin. For the current study, the preheated air is mixed with superheated steam upstream of the injectors. The cylindrical combustion chamber is made from quartz glass in order to have optical access to the flame, and is followed by a water-cooled exhaust tube. The test rig is operated at atmospheric conditions. For the current study, natural gas, hydrogen, and various mixtures of both gases are used as fuel. The methane concentration in the natural gas is above 98%.

Exhaust gas is extracted at several radial positions 850 mm downstream of the burner outlet with a water-cooled probe, and transported through a heated tube to a cold steam trap to remove humidity. It is then analyzed for CO, NO, NO<sub>2</sub>, O<sub>2</sub>, and CO<sub>2</sub> on a dry basis. The species concentrations on a wet basis are calculated from the known operating conditions. A cooled sampling probe with a single hole can be traversed to measure local gas concentrations.

An intensified CCD camera with a bandpass filter at 308 nm is used to measure the spatial distribution of the OH\* chemiluminescence. This signal correlates with the heat release and is used to identify the shape and anchoring position of the flame.

Throughout the study, the steam content is described by the steam-to-air mass ratio

$$\Omega = \frac{\dot{m}_{steam}}{\dot{m}_{air}}, \quad (1)$$

where  $\dot{m}_{steam}$  is the mass flow rate of steam, and  $\dot{m}_{air}$  the mass flow rate of air. The equivalence ratio  $\phi$  is used to describe the fuel concentration. It is defined as

$$\phi = \frac{\dot{m}_{fuel}/\dot{m}_{air}}{(\dot{m}_{fuel}/\dot{m}_{air})|_{st}}, \quad (2)$$

where  $\dot{m}_{fuel}$  and  $\dot{m}_{air}$  are the mass flow rates of fuel and air, and  $(\dot{m}_{fuel}/\dot{m}_{air})|_{st}$  is the stoichiometric mass fraction for the given fuel. It is 0.58 for methane, and 0.029 for hydrogen. The equivalence ratio  $\phi$  is smaller than 1 for lean conditions, and larger than 1 for rich conditions.

The premixed combustor is presented in Fig. 1a. It provides a nearly homogeneous mixture of fuel, air and steam at the burner outlet. For the current study, the injector is set to a constant geometric swirl number of  $S = 0.7$ . The swirl number is generally defined as the ratio of the axial flux of the tangential momentum to the axial flux of the axial momentum, normalized with the combustor radius. For the generic burner, the swirl number can also be determined from the geometry of the swirl generator and the mixing tube [14].

The combustion chamber of the lean premixed combustor is made from quartz glass and has a length of 300 mm and a diameter of 200 mm. The combustor has four ports at axial locations between 50 mm (referred to as port 1) and 200 mm (port 4) which are used for local temperature and gas concentration measurements. The quartz glass is followed by a water-cooled exhaust tube with a length of 760 mm. The combustor inlet temperature is measured in the mixing tube of the burner, downstream of the fuel injection. It is controlled in order to have a deviation of the set value of less than  $\pm 3$  K.

The total mass flow rate of air plus steam is kept constant at  $\dot{m} = 180$  kg/h. Depending on the equivalence ratio, the thermal power of the combustor is between 75 and 150 kW. The combustor inlet temperature is varied between 293 K and 623 K. Natural gas (NG), hydrogen, and volumetric mixtures of 53%NG/47%H<sub>2</sub> and 33%/67% are used as fuel for the combustion tests. For a typical measurement series, the inlet temperature and mass flow rates of air and steam are kept constant, and the equivalence ratio is decreased from  $\phi = 0.95$  to the lean blowout limit in steps of  $\Delta\phi = 0.05$ .

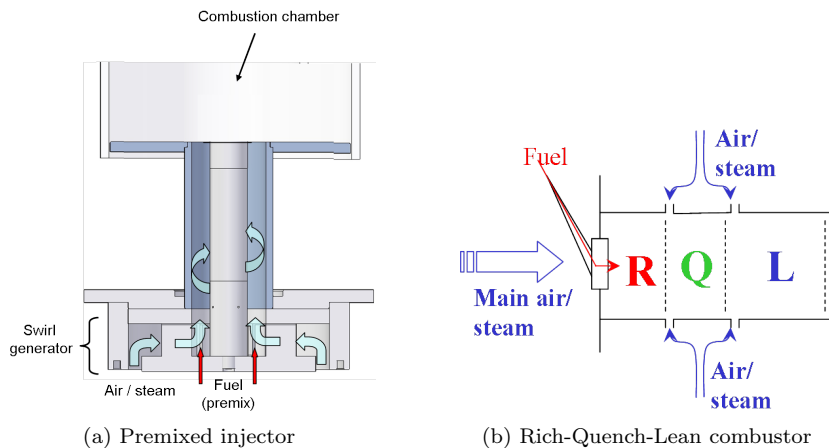


Figure 1: Combustion systems.

The schematic of the Rich-Quench-Lean (RQL) combustor is shown in Fig. 1b. An industrial injector is used which has three axial swirl generators. The fuel is injected between the inner and the intermediate swirler. Additional air/steam is injected into the quenching (Q) and the dilution (L) zone through eight circumferential chutes each, which are connected to the plenum upstream of the injector. Approximately 23% of the total flow enter the rich zone through the injector, 24% are injected into the quenching zone, and the remaining 53% into the dilution zone. To ensure a constant flow distribution throughout the experiments, the flow split is determined by measuring the pressure drops and controlled with valves. The combustion chamber has a diameter of 105 mm and a length of 350 mm, followed by a water-cooled exhaust tube with a length of 760 mm. Quartz glasses are used for the rich zone and the dilution zone. The injector inlet temperature is measured in the plenum directly upstream of the injector, the temperatures of the quenching and dilution flows are measured in the manifolds surrounding the chutes.

The combustor is operated at a constant pressure drop of the injector of approximately 4%, which leads to total mass flow rates of air and steam between  $\dot{m} = 250$  kg/h and 300 kg/h. Measurements are conducted at inlet

temperatures of 500 K, 600 K, and 650 K. Natural gas, hydrogen, and volumetric mixtures of 90%NG/10%H<sub>2</sub> and 50%/50% are used as fuel. The combustor is typically operated at constant inlet temperature and steam content, while the global equivalence ratio is decreased in small steps from  $\phi = 0.7$  until the flame blows out. For high steam content, the operational range can be additionally restricted by rich blowout. This leads to a thermal power between 25 kW and 200 kW. The local equivalence ratio in the rich zone,  $\phi_{RZ}$ , has a strong influence on the combustion process and is used in the discussion of the results. It can be estimated from the combustor flow splits as  $\phi_{RZ} = 0.23\phi$ .

### 3. Modeling

Chemical reactor networks (CRN) are designed to model the combustion process of the two tested systems and to gain a detailed insight into the NO<sub>x</sub> and CO formation at wet conditions. The models consist of a number of perfectly stirred reactors (PSR); the schematics are shown in Fig. 2. The network layouts and parameters, such as reactor volumes, flow splits, and recirculation rates, remain the same for all simulations; changes in the flow field between different operating conditions are not included in the models.

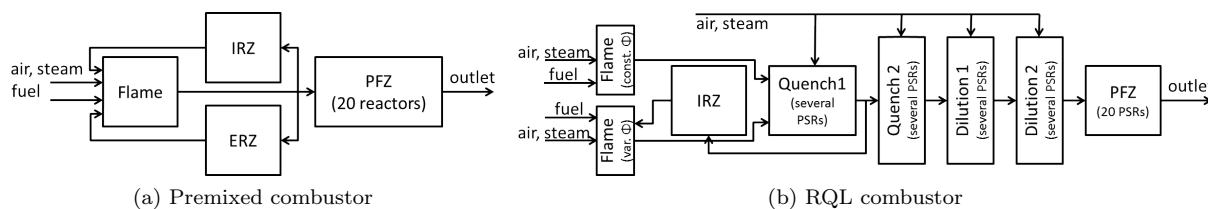


Figure 2: Chemical reactor networks.

The reactor network for the premixed combustor is based on a study published recently [11]. It represents the main regions of the flow field of the swirl-stabilized combustor: the main flame zone (MFZ) comprising the inlet jet or flame, the external recirculation zone (ERZ), and the inner recirculation zone (IRZ). Each zone is modeled with a single PSR. Additional reactors to simulate the effect of incomplete fuel-air mixing are not added, since the mixing quality of the generic burner is very high [15]. The reactor volumes are estimated from OH\* chemiluminescence images of a typical flame at dry conditions (Fig. 3 in the following Section 4). The recirculation rates for the IRZ and the ERZ are estimated from the non-reacting flow field [11]. The main flame zone is followed by the post-flame zone (PFZ), extending from the flame to the location of the gas sampling probe in the experimental set up. It is modeled by a series of 20 PSRs, approximating a plug-flow reactor. Radiative heat loss is included for the flame reactor with an optical thin model [16]. The convective heat transfer of the flame reactor is calculated from a correlation derived from local flame temperature measurements. The correlation is a function of the heat capacity, the thermal conductivity, and the temperature of the gas. Heat transfer of the post-flame zone is calculated from the temperature of the cooling water of the exhaust tube for each measurement point. The flame reactor has a mean residence time  $\tau = V_{PSR}/\dot{V}_{PSR}$  between 2.7 ms and 3.7 ms, depending on temperature and degree of dilution. The total residence time of the complete network varies between 65 ms and 95 ms. This is relatively long compared to current commercial gas turbine combustors, however, the conclusions drawn in the current study remain valid also for shorter residence times of around 15 ms. The network simulations show that longer residence times only have a marginal influence on the NO<sub>x</sub> and CO formation.

The reactor network for the RQL combustor is more complex. In contrast to the nearly homogeneous fuel-air-steam mixture of the premixed combustor, the fuel is now injected directly into the combustion chamber, which leads to a relatively broad distribution of local equivalence ratios at the location of the flame. This is taken into account by modeling the flame with several perfectly stirred reactors of fixed and variable stoichiometry. The inner recirculation zone consists of a single PSR. It is followed by several PSRs for the quenching zone. Steam and air are injected at two axial locations to simulate a more gradual

mixing with the reaction products. Some of the gas of the first quenching reactors is recirculated through the IRZ into the flame reactors. The dilution zone is again modeled by several PSRs with injection of the air and steam at two axial locations. All these reactors constitute the main flame zone, which is followed by 20 PSRs for the post-flame zone. The complete reactor network consists of 43 perfectly stirred reactors. Heat loss due to gas radiation is modeled using an optical thin model for the flame reactors [16] and the gray-band model by Leckner [17] for the remaining reactors of the main flame zone, estimating the optical mean path lengths from the reactor volumes. Convective heat transfer between the reactors of the MFZ and the environment is simply assumed to be proportional to the gas temperature; the coefficients remain the same for all simulations. Heat transfer in the post-flame zone is calculated in the same manner as for the premixed combustion model. The same reactor network is used for all operating conditions and fuel compositions. The mean residence time of the flame zone is between 2.9 ms and 3.3 ms. The total residence time in the combustor varies between 20 ms and 45 ms.

The reactor networks are implemented using the software *Cantera* [18]. Two different reaction mechanisms are used: the GRI-Mech 3.0 mechanism [19] for the simulations of the pure hydrogen flames, and the “Detailed reaction mechanism for small hydrocarbons combustion, Release 0.5” by Konnov [20] for the methane-containing fuels. The role of the individual  $\text{NO}_x$  formation pathways is investigated by disabling the corresponding reaction equations. The difference to the  $\text{NO}_x$  concentrations obtained with the unchanged mechanism is attributed to the specific pathway. For the operating conditions investigated, the influence of the deactivation of these reactions on autoignition times and burning velocities are negligible. In order to further reduce a possible influence of these effects, the  $\text{NO}_x$  formation pathways are evaluated at the reactor temperatures of the original reaction mechanisms. This approach works well, and the different pathways add up to more than 95% of the total  $\text{NO}_x$  concentration calculated with the original reaction mechanisms.

## 4. Results

### 4.1. Influence of Steam on Flame Shape

In the following, the general influence of steam dilution on the flame shape and position is discussed based on the premixed combustor. The Abel deconvoluted  $\text{OH}^*$  chemiluminescence images and local concentrations of carbon monoxide for typical premixed flames at dry and at wet conditions are presented in Fig. 3. In order to achieve the same adiabatic flame temperatures, the inlet temperature and the equivalence ratio are changed.

The combustor flow field is characteristic for swirl-stabilized flames and consists of three distinct regions: The annular jet emanating from the mixing tube, the internal recirculation zone generated by the vortex breakdown, and the external recirculation zone.

At dry conditions, a v-shaped flame is observed in the experiments with natural gas, which is typical for such a premixed, swirl-stabilized combustor. The flame is located between the inlet jet and the inner recirculation zone and is relatively compact. At wet conditions, the flame speed is reduced and the reaction rates are lower, which leads to a wider reaction zone and moves the maximum of the  $\text{OH}^*$  radiation and CO concentration further downstream and closer to the combustor walls. At a steam-air ratio of  $\Omega = 30\%$ , the natural gas flame is distributed over a relatively wide range. A substantial further increase in steam content is only possible if the combustor inlet temperature is also increased. Up to these high degrees of steam dilution, CO concentrations are not noticeably higher.

With increasing hydrogen content in the fuel, the flame becomes significantly shorter and the effect of the added steam on the flame position and length is lower. The flame can also sustain higher strain and is located along the shear layers towards the inner as well as the outer recirculation zone. The maximum possible steam content increases with hydrogen content; for pure hydrogen fuel and a moderate inlet temperature of 623 K, the flame can sustain levels of steam dilution up to  $\Omega = 50\%$ .

The RQL combustor also has a swirl-stabilized flame with an inner recirculation zone in the rich zone. The influence of steam and fuel content are similar as for the premixed system: With increasing steam content, the flame becomes less compact and is located further downstream from the injector (Fig. 4).

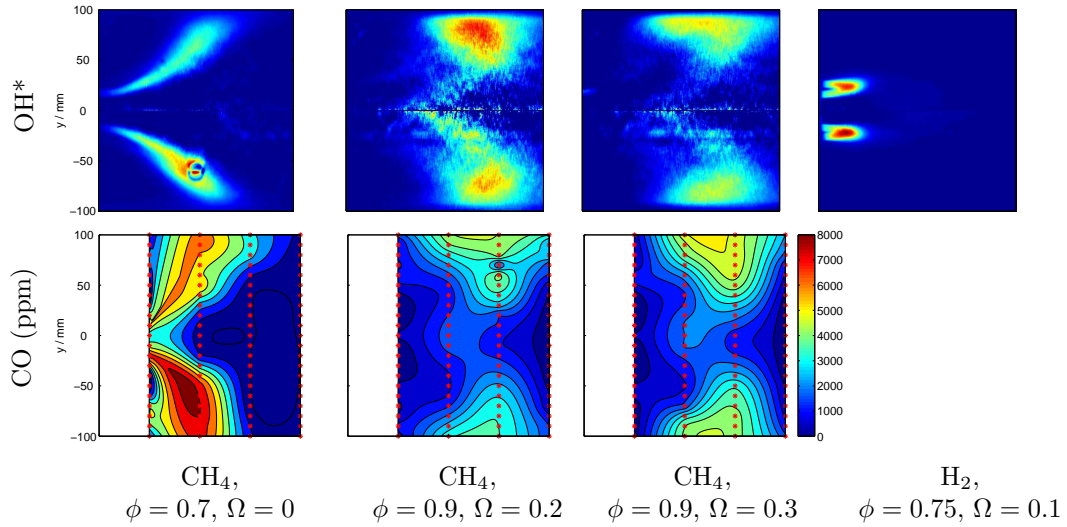


Figure 3: Abel deconvoluted  $\text{OH}^*$  chemiluminescence and local gas concentrations for the premixed combustion system. Adiabatic flame temperatures between 1560 K and 1600 K. (Injector outlet on the left side. Measurement locations indicated by red crosses.)

Increasing the hydrogen content in the fuel stabilizes the flame again: The flame becomes more compact and can sustain higher steam contents. For the inlet temperature of 650 K, the maximum possible steam-air mass ratio achieved in the experiments is  $\Omega = 25\%$  for natural gas, and approximately  $\Omega = 35\%$  for hydrogen.

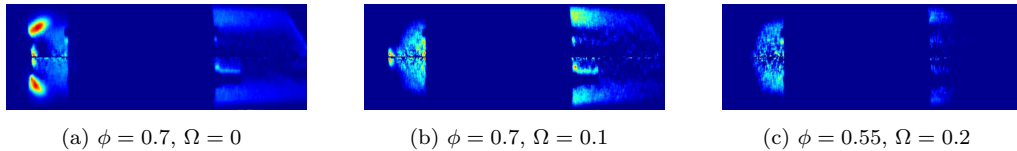


Figure 4: Abel deconvoluted  $\text{OH}^*$  chemiluminescence images of the RQL combustor. Rich zone is on the left, dilution zone on the right, the quenching zone is hidden by the injection manifold. (NG,  $T_{in} = 650$  K)

Due to the higher local equivalence ratios, the RQL combustor has improved lean blowout limits compared to the premixed combustor; flame extinction occurs at lower equivalence ratios. For operation on natural gas, the lean blowout limit of the RQL system increases from  $\phi = 0.16$  at dry conditions to  $\phi = 0.27$  at 20% steam content ( $T_{in} = 650$  K), whereas it increases from  $\phi = 0.44$  to  $\phi = 0.64$  for the premixed flame ( $T_{in} = 623$  K). The operational range of the RQL system, however, is additionally limited by rich blowout at wet conditions. For a steam content of  $\Omega = 20\%$ , the maximum equivalence ratio achieved in the experiments is  $\phi = 0.56$ .

#### 4.2. CO Formation

The CO emissions from the measurements and from the simulations are presented in Fig. 5, exhibiting the typical trends of the assessed combustion systems.

The simulation results show an excellent agreement with the experimental data for both combustors, and accurately predict the influence of equivalence ratio and steam content. The small differences to the experimental results are caused by slightly different gas temperatures to which CO is very sensitive. At 20%

steam content, the flame in the RQL combustor is moved relatively far downstream in the experiments, and is located behind the quenching and dilution ports. This leads to changes in the flow field which are not reflected in the network design, and the model predicts a more narrow operational range at these conditions.

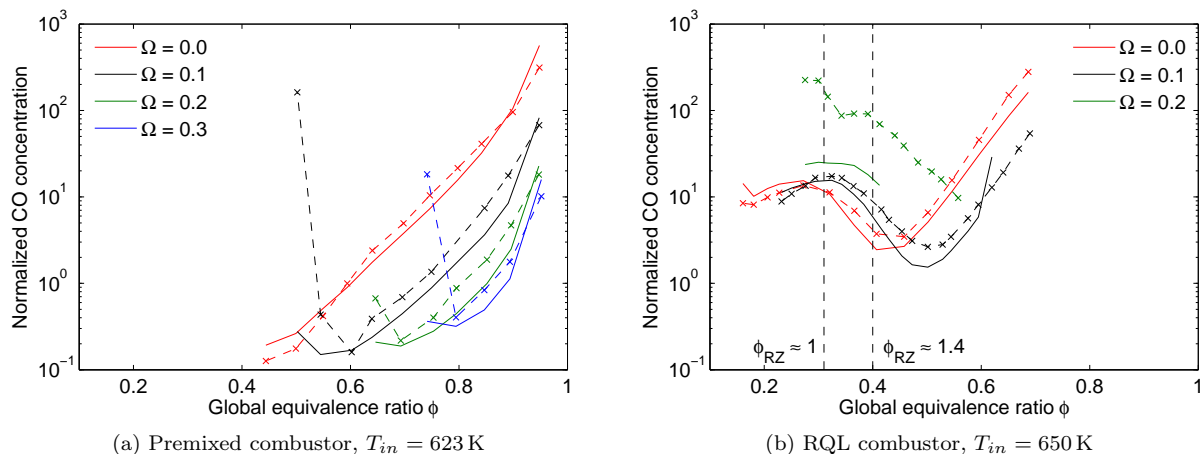


Figure 5: CO emissions for natural gas. Experimental data ( $-x-$ ) and simulation results ( $-$ ). Data normalized with the value of the premixed combustor at  $\phi = 0.6$ ,  $\Omega = 0$ .

At dry conditions, the lowest CO emissions in the premixed combustor are achieved for low equivalence ratios around  $\phi = 0.5$ . With increasing fuel content, the CO concentrations follow the trend of the chemical equilibrium which is determined by the gas temperature and carbon content. At very low equivalence ratios near the lean blowout limit, the emissions can increase due to low gas temperatures which restrain the kinetics of the CO burnout. In the reactor network, heat release and CO burnout occur mostly in the flame reactor. The remaining CO is oxidized in the recirculation reactors and in the first reactors of the post-flame zone.

In the RQL combustor, the CO formation is largely determined by the local equivalence ratio in the rich zone. At lean conditions in the rich zone, the CO formed in the flame has no sufficient residence time for the burnout before cold gases are injected in the quenching zone. This leads to high CO emissions with a local maximum around  $\phi_{RZ} = 1$ . For higher equivalence ratios, the remaining fuel burns in the quenching zone, when additional oxygen is available again. This leads to a temperature increase in this zone, and, thus, to improved CO burnout. The temperatures of the different reactor zones are presented in Fig. 6. The lowest CO emissions are achieved at a global equivalence ratio of  $\phi = 0.4$ , where the temperature distribution is relatively even and beneficial for the CO burnout. For even higher equivalence ratios, CO increases again and follows the chemical equilibrium. At these conditions, the CO is higher than in the premixed combustor mainly due to higher exhaust temperatures. In gas turbines, the RQL combustor is typically operated around  $\phi = 0.4$ , just before CO increases with the chemical equilibrium.

At moderately wet conditions, the CO emissions of both combustion systems exhibit the same trends as at dry conditions, but are moved towards higher equivalence ratios. This is mostly caused by the reduced temperatures at these conditions, leading to lower CO concentrations at the chemical equilibrium and to an earlier increase at lean conditions. In literature, increasing CO emissions are frequently reported already at moderately humid conditions, which is explained by flame instabilities and local quenching [10, 21]. In the current study, relatively high CO emissions are also observed for the RQL combustor at 20% steam content. At these operating conditions, the heat release is mostly located downstream of the dilution ports. In addition to increased local extinction and the flame being less stable, the residence time to the combustor exit is reduced, which all leads to the increased CO emissions. In the premixed combustor, these effects do not occur and single-digit CO emissions are achieved even up to ultra-wet conditions.

The simulation results agree well with the experimental data. An influence of the steam on the CO emissions via changes in the OH concentration seems to be negligible. At increased pressure, this behaviour could possibly change due to the increased third body collision efficiency of water [7].

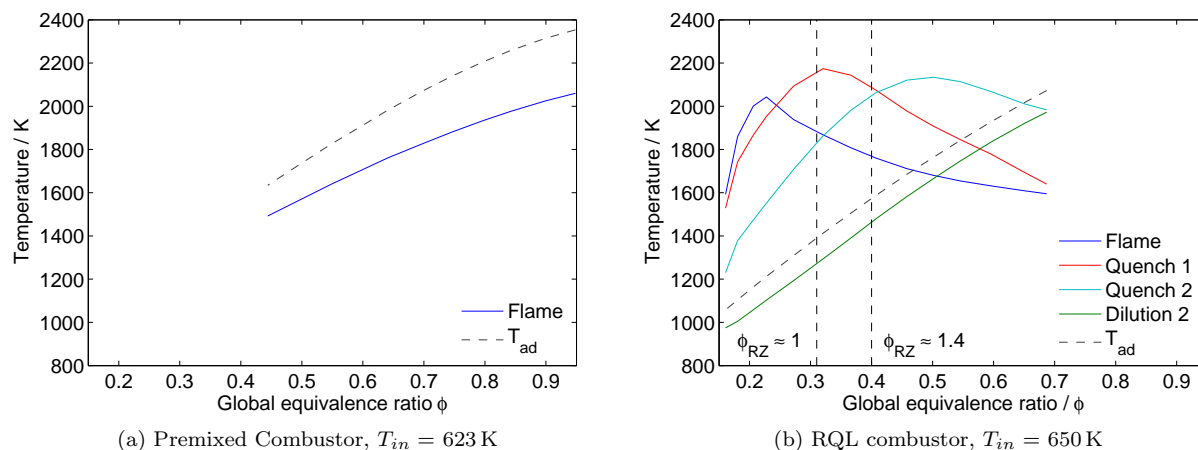


Figure 6: Average temperatures of the reactor network zones for operation with natural gas at dry conditions.

### 4.3. NO<sub>x</sub> Formation

In the following, the measured NO<sub>x</sub> emissions are presented and discussed along with the simulation results. In the subsequent section, the reactor networks are used for a more detailed investigation of the NO<sub>x</sub> formation and the role of the different pathways.

#### 4.3.1. Premixed Combustor

At dry conditions, the measured NO<sub>x</sub> emissions for the natural gas flame are relatively low for very lean operating points, but increase rapidly with increasing equivalence ratio and temperature (Fig. 7a). This limits current premixed gas turbine combustors to these lean conditions with low temperatures. With increasing hydrogen content in the fuel, NO<sub>x</sub> emissions increase for a constant equivalence ratio due to higher flame temperatures (Fig. 7c for pure hydrogen). For the same flame temperature, hydrogen content does not noticeably lead to higher NO<sub>x</sub> emissions.

At wet conditions, NO<sub>x</sub> emissions are significantly reduced for natural gas as well as for hydrogen. This is the case also for the same flame temperature, when the equivalence ratio is increased to compensate for the higher heat capacity of the added steam. For all tested fuels, emissions are well below 10 ppm (at 15% O<sub>2</sub>, dry) up to near-stoichiometric conditions for steam contents above  $\Omega = 20\%$ . For steam-air ratios above 20%, pure hydrogen leads to lower NO<sub>x</sub> emissions than natural gas even at the same equivalence ratio and corresponding higher flame temperature. This higher effectivity of steam dilution for NO<sub>x</sub> reduction in the hydrogen flame is explained in a recent study [9], which found that the CH-dependant prompt pathway is less restrained by the steam than the other pathways. In this recent study, the NO<sub>x</sub> emissions were measured for different flame temperatures (Fig. 8), revealing the chemical influence of the steam on the NO<sub>x</sub> formation.

Figures 7a and 7c also present the simulation results obtained with the reactor network. Without dilution, the predicted NO<sub>x</sub> emissions for natural gas agree well with the experimental data over the whole range of equivalence ratios and inlet temperatures. For the hydrogen flame, the deviation from the experimental values increases slightly at very lean equivalence ratios, but this is less than 1 ppm. At wet conditions, the simulation results are in excellent agreement with the experimental data for all fuels investigated.

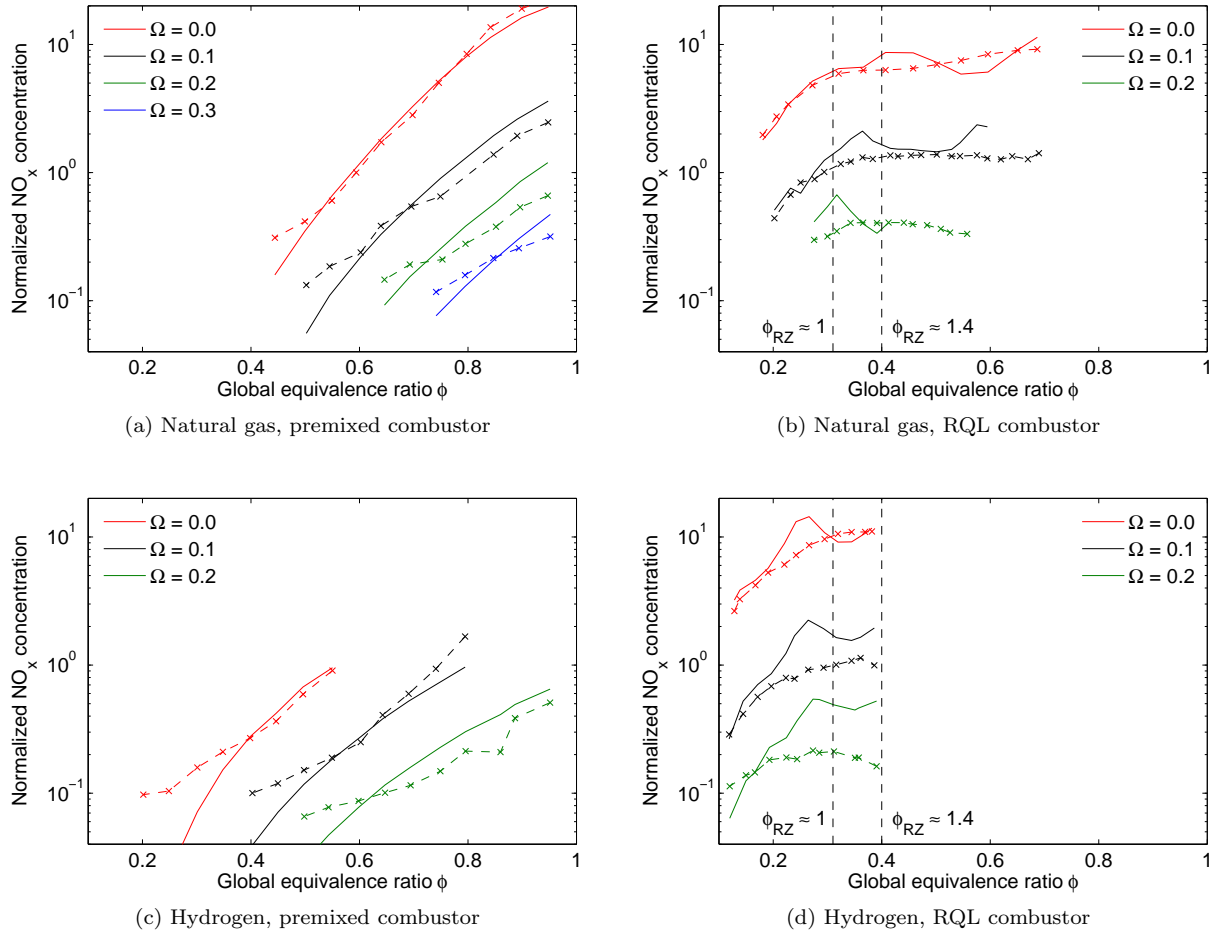


Figure 7:  $\text{NO}_x$  emissions for natural gas and hydrogen. Experimental data ( $-x-$ ) and simulation results ( $-$ ). Data normalized with the value of the premixed combustor at  $\phi = 0.6$ ,  $\Omega = 0$ .

#### 4.3.2. Rich-Quench-Lean Combustor

The measured  $\text{NO}_x$  emissions for the RQL combustor are presented in Fig. 7b and 7d for natural gas and hydrogen fuel.

At dry conditions and operation on natural gas,  $\text{NO}_x$  emissions increase rapidly with increasing equivalence ratio at very lean conditions. At a global equivalence ratio of around  $\phi = 0.3$ , the mixture in the rich zone reaches stoichiometric conditions ( $\phi_{RZ} \approx 1$ ) and the local  $\text{NO}_x$  production reaches its maximum. For higher equivalence ratios – for which the rich-quench-lean concept is designed – the  $\text{NO}_x$  formation in the rich zone declines again, and the total  $\text{NO}_x$  emissions remain approximately constant. A local minimum is reached around  $\phi = 0.4$ , when the equivalence ratio in the rich zone is approximately  $\phi_{RZ} = 1.4$  and the concentrations of NO and its precursors HCN and  $\text{NH}_3$  are the lowest. This effect is more pronounced at increased pressure [22]. Similarly as for the premixed combustor,  $\text{NO}_x$  emissions increase with increasing hydrogen content in the fuel due to the higher flame temperature at the same equivalence ratio. The general trends remain the same.

With steam dilution,  $\text{NO}_x$  emissions are significantly lower for both fuels. At a steam-air mass ratio of 20%, the hydrogen flame again leads to lower  $\text{NO}_x$  emissions than the natural gas flame due to the inexistent prompt pathway. At this steam content,  $\text{NO}_x$  emissions well below 10 ppm are measured for all fuels and

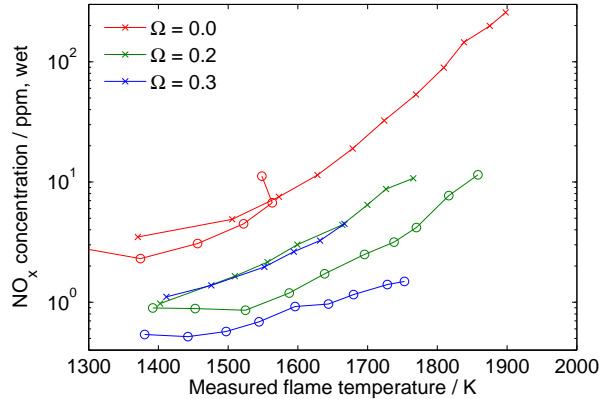


Figure 8: Measured  $\text{NO}_x$  concentration and flame temperature in the premixed combustor [9]. Operation with natural gas ( $\text{---}\times\text{---}$ ) and hydrogen ( $\text{---}\circ\text{---}$ ). The equivalence ratio was decreased from  $\phi = 0.95$  (dry  $\text{H}_2$  flame from  $\phi = 0.55$ ) to blowout for each curve.

all operating conditions investigated.

The reactor network accurately predicts the  $\text{NO}_x$  emission trends for the different fuels, steam contents, and inlet temperatures. At very lean conditions, an excellent agreement with the experimental data is achieved, whereas for higher equivalence ratios, the predicted emissions deviate slightly from the measurement results. Particularly for operation on hydrogen and at wet conditions,  $\text{NO}_x$  formation is over-predicted. This is probably caused by changes in the flow field due to different flame positions and by the increased heat loss at wet conditions which is not correctly predicted by the simple heat model of the reactor network.

Compared to the  $\text{NO}_x$  emission levels of the premixed injector, the RQL combustor generally leads to higher absolute emissions. This is partly caused by the experimental setup: The better thermal insulation due to the surrounding injection manifold and the short quartz glasses reduces the heat loss and thus increases the gas temperatures. The main reason for the higher  $\text{NO}_x$  emissions, however, is inherent to the RQL approach which leads to significantly higher local temperatures than in the premixed combustor (Fig. 6).

#### 4.4. $\text{NO}_x$ Formation Pathways

The effect of steam injection on the  $\text{NO}_x$  emissions through the different formation pathways is investigated in the following, using the reactor networks with the detailed reaction mechanisms.

Four major pathways contribute to the formation of  $\text{NO}_x$  in combustion processes. They are distinguished by the reaction of molecular nitrogen  $\text{N}_2$  into atomic nitrogen  $\text{N}$ , which requires high activation energies and thus is the rate-limiting step.  $\text{NO}_x$  formation through the prompt,  $\text{N}_2\text{O}$ , and  $\text{NNH}$  pathways requires only short residence times and mostly occurs within the main region of heat release, the flame. The thermal pathway requires relatively long residence times and high temperatures and is usually more important in the hot post-flame regions of a combustor. In addition to temperature, the pathways also depend strongly on the concentrations of reactive intermediate species. The prompt pathway requires  $\text{CH}_x$  radicals to attack the molecular nitrogen and hence is only relevant for carbon-containing fuels. The other three pathways depend on the concentrations of atomic hydrogen  $\text{H}$ , atomic oxygen  $\text{O}$ , and the hydroxyl radical  $\text{OH}$ . The influence of steam on these species and the  $\text{NO}_x$  formation has recently been investigated for the premixed combustion system for different fuel mixtures of methane and hydrogen [9]. It was shown that in addition to the potential flame temperature reduction, the steam directly affects the  $\text{NO}_x$ -chemistry. The concentrations of  $\text{OH}$  and  $\text{H}$  change only slightly with the steam content, whereas the  $\text{O}$  concentration is significantly reduced, thus restraining the thermal,  $\text{N}_2\text{O}$ , and the  $\text{NNH}$  pathways. For methane-containing fuels, steam injection can lead to slightly increased  $\text{CH}$  radical concentrations, thus increasing the  $\text{NO}_x$  formation through the prompt pathway.

The contribution of the different formation pathways on the total  $\text{NO}_x$  emissions is presented in Fig. 9 for selected operating points for the two combustion systems.

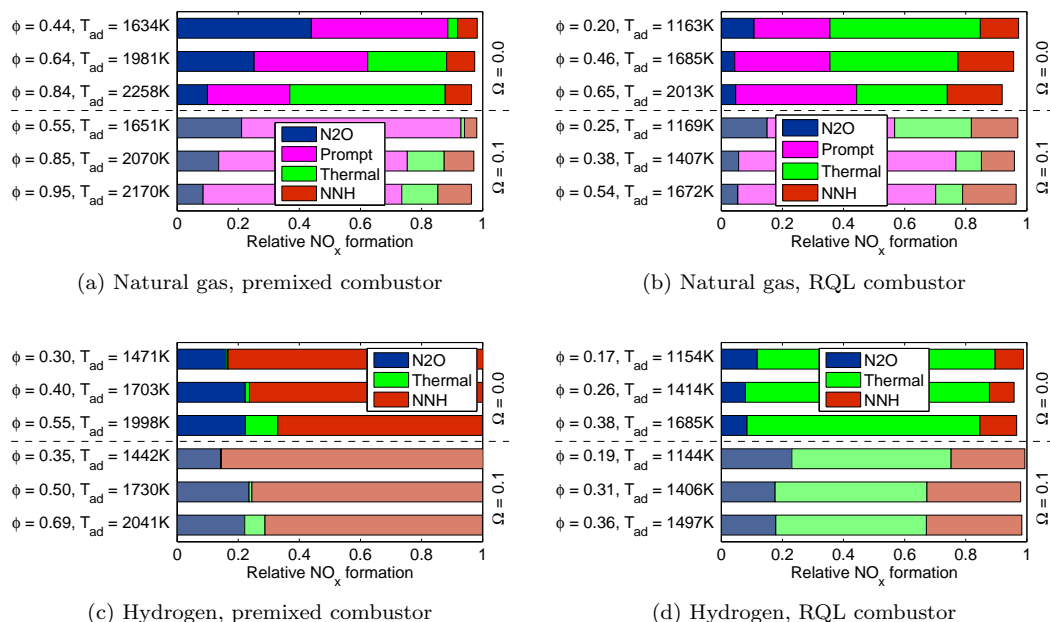


Figure 9: Contribution of the formation pathways to the total  $\text{NO}_x$  emissions.

In the premixed combustor,  $\text{NO}_x$  is mainly formed in the flame reactor, and only very little  $\text{NO}_x$  is produced in the two recirculation reactors due to the relatively low temperatures. For the undiluted natural gas flame, the reactor network predicts the results which are to be expected for this combustion system. At lean conditions, the  $\text{N}_2\text{O}$  and prompt pathways are relatively strong, whereas the thermal pathway is negligible. For flame temperatures above 1800 K, the thermal pathway dominates the overall  $\text{NO}_x$  formation. For the steam-diluted natural gas flame, the individual contributions of the formation pathways change significantly. With increasing steam content, the NNH, the  $\text{N}_2\text{O}$ , and the thermal pathway are restrained and produce substantially less  $\text{NO}_x$ , even for the same flame temperature. In contrast,  $\text{NO}_x$  formation through the prompt pathway is increased at wet conditions. This comes from the higher CH radical concentrations due to the increased equivalence ratio required to make up for the higher heat capacity of the added steam.

For the dry, premixed hydrogen flame,  $\text{NO}_x$  formation is dominated by the NNH pathway due to high H atom concentrations. With increasing steam content, all three pathways are restrained considerably, while the relative pathway contributions remain similar.

The  $\text{NO}_x$  production of the individual zones of the RQL reactor network is presented in Fig. 10. At low equivalence ratios and dry conditions,  $\text{NO}_x$  is mostly formed in the flame reactors. As the  $\text{NO}_x$  production depends directly on the temperature (Fig. 6) and the concentrations of intermediate species,  $\text{NO}_x$  is increasingly formed also in the quenching and dilution reactors for higher equivalence ratios and steam contents. In these regions, high concentrations of H and CH radicals occur during the breakdown of the fuel, leading to a strong contribution of the NNH and the prompt formation pathways. For the natural gas flame,  $\text{NO}_x$  re-burn occurs to a certain degree in the first reactors of the quenching zone, where gas from the flame with high temperature and high  $\text{NO}_x$  concentrations is diluted with air to form a slightly rich mixture, creating beneficial conditions for the  $\text{NO}_x$  re-burn. For the hydrogen flame, the thermal pathway is particularly strong. The heat release of this compact flame occurs very early in the combustor, giving the reaction products a long residence time at high temperatures to form thermal  $\text{NO}_x$ .

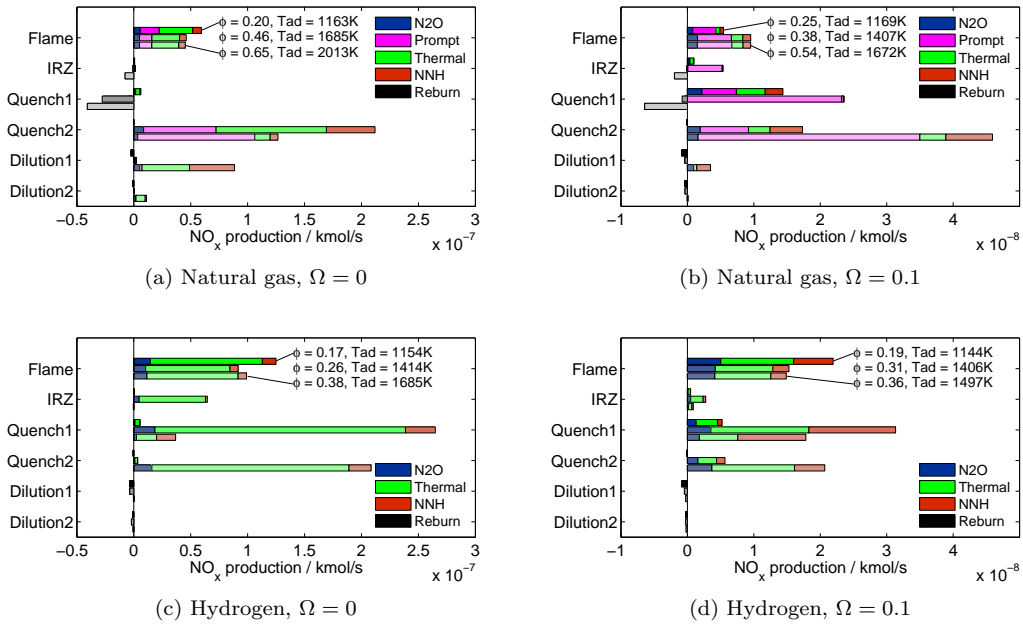


Figure 10:  $\text{NO}_x$  production in different reaction network zones of RQL combustor ( $T_{in} = 650 \text{ K}$ ).

At dry conditions, the simulations of the RQL combustor predict for both fuels a noticeably higher share of the thermal pathway compared to the premixed flame (Fig. 9), which is caused by the high local temperatures already at low equivalence ratios. For the natural gas flame, the prompt  $\text{NO}_x$  formation increases with the equivalence ratio. At wet conditions, the prompt pathway is dominating overall  $\text{NO}_x$  formation also for the RQL combustor. Again, the increased fuel content required to achieve the same temperatures, and the adverse influence of the steam, lead to higher CH radical concentrations and to an increased  $\text{NO}_x$  production through this pathway. The inherent strong role of the prompt pathway in the RQL combustor thus could potentially reduce the effectivity of the steam dilution on  $\text{NO}_x$  reduction for the natural gas flame. All three relevant pathways of the hydrogen flame are significantly restrained at wet conditions, leading to the lower measured  $\text{NO}_x$  emissions than for natural gas at high steam contents.

## 5. Conclusions

The combustion of natural gas and hydrogen was investigated for a premixed and a Rich-Quench-Lean combustor with high degrees of steam dilution. CO and  $\text{NO}_x$  emissions, local species concentrations, and flame shape and position were measured in combustion tests at atmospheric conditions. Two reactor networks were designed and validated with the experimental results.

For operation on natural gas and a moderate inlet temperature around 650 K, a stable flame was achieved up to 30% steam content with the premixed combustor, and 20% with the RQL combustor. The operational range of his combustor was additionally restricted by rich blowout at wet conditions. Significantly higher steam contents are possible with hydrogen fuel. The risk of flashback for the hydrogen-containing fuels was lower in the presence of steam, and pure hydrogen fuel could be burnt in the premixed combustor up to stoichiometric conditions already at the lowest assessed steam-to-air mass ratio of 10%.

The measured  $\text{NO}_x$  emissions were significantly reduced at wet conditions: For steam contents above 20%,  $\text{NO}_x$  emissions below 10 ppm were achieved with both combustion systems for operation on natural gas and hydrogen even at highest temperatures and equivalence ratios investigated. Steam injection thus enables operation of RQL systems at very low  $\text{NO}_x$  emissions and with high fuel flexibility.

The measured CO emissions were not noticeably affected for moderate degrees steam dilution and remained on a low level. For high steam contents of 20% or higher, CO was increased for the RQL combustor for lean conditions, whereas it remained low for the premixed system.

The reactor networks are capable of predicting NO<sub>x</sub> and CO emissions with good agreement to the experimental results for dry and wet conditions. They were used to gain a detailed understanding of the NO<sub>x</sub> formation. At dry conditions, the thermal pathway is dominant already at low equivalence ratios in the RQL combustor due to high local temperatures. For the premixed combustor operating at dry conditions, the prompt pathway is strong for natural gas, and the NNH pathway for hydrogen combustion. At wet conditions, the prompt pathway becomes dominant in both combustion systems for operation on natural gas, whereas the other three pathways are significantly constrained. This also leads to the observed higher effectivity of steam injection for NO<sub>x</sub> reduction for the hydrogen flame.

## Acknowledgements

The authors would like to thank Andy Göhrs and Phoebe Kuhn for their support. The research leading to these results has received funding from the European Research Council under the ERC grant agreement n° 247322, GREENEST. The project received funding from Rolls-Royce Canada.

## References

- [1] Pratt & Whitney, Humid air turbine cycle technology development program - final report, Technical progress report, National Energy Technology Center U.S. Department of Energy (July 2002).
- [2] A. K. Das, K. Kumar, C. Sung, Laminar flame speeds of moist syngas mixtures, 2010. doi:10.1016/j.combustflame.2010.09.004.
- [3] E. Gurentsov, O. Divakov, A. Eremin, Ignition of multicomponent hydrocarbon/air mixtures behind shock waves, High temperature 40 (3) (2002) 379–386.
- [4] A. Mazas, D. Lacoste, T. Schuller, Experimental and numerical investigation on the laminar flame speed of ch<sub>4</sub>/o<sub>2</sub> mixtures diluted with co<sub>2</sub> and h<sub>2</sub>o, in: ASME Turbo Expo 2010, ASME Paper 2010-GT-22512, 2010.
- [5] A. Frassoldati, T. Faravelli, E. Ranzi, A wide range modeling study of nox formation and nitrogen chemistry in hydrogen combustion, International Journal of Hydrogen Energy 31 (2006) 2310–2328.
- [6] F. Dryer, Water addition to practical combustion systems - concepts and applications, 16<sup>th</sup> International Symposium on Combustion, The Combustion Institute.
- [7] D. Zhao, H. Yamashita, K. Kitagawa, N. Arai, T. Furuhashi, Behavior and effect on NO<sub>x</sub> formation of OH radical in methane-air diffusion flame with steam addition, Combustion and Flame 130 (2002) 352–360. doi:10.1016/S0010-2180(02)00385-1.
- [8] A. Bhargava, M. Colket, W. Sowa, K. Casleton, D. Maloney, An experimental and modeling study of humid air premixed flames, Journal of Engineering for Gas Turbines and Power 122 (2000) 405–411. doi:10.1115/1.1286921.
- [9] S. Göke, C. O. Paschereit, Influence of steam dilution on NO<sub>x</sub> formation in premixed natural gas and hydrogen flames, in: 50<sup>th</sup> AIAA Aerospace Science Meeting, AIAA-2012-1272, 2012.
- [10] T. Le Cong, P. Dagaut, Effect of water vapor on the kinetics of combustion of hydrogen and natural gas: experimental and detailed modeling study, in: ASME Turbo Expo 2008, ASME Paper 2008-GT-50272, 2008.
- [11] S. Göke, S. Terhaar, K. Göckeler, C. Paschereit, Combustion of natural gas, hydrogen and bio-fuels at ultra-wet conditions ASME Turbo Expo 2011, ASME Paper 2011-GT-45696.
- [12] H. Kobayashi, S. Yata, Y. Ichikawa, Y. Ogami, Dilution effects of superheated water vapor on turbulent premixed flames at high pressure and high temperature, Proceedings of The Combustion Institute 32 (2009) 2607–2614.
- [13] J. Park, S. I. Keel, J. H. Yun, Addition effects of h<sub>2</sub> and h<sub>2</sub>o flame structure and pollutant emissions in methane-air diffusion flame, Energy and Fuels 21 (2007) 3216–3224. doi:10.1021/ef700211m.
- [14] C. Schneider, Ueber die charakterisierung von turbulenzstrukturen in verdrahteten strömungen, Ph.D. thesis, Technische Universität Darmstadt (2003).
- [15] S. Göke, K. Göckeler, O. Krüger, C. Paschereit, Computational and experimental study of premixed combustion at ultra wet conditions, in: ASME Turbo Expo 2010, ASME Paper 2010-GT-23417, 2010.
- [16] R. Barlow, A. Karpetis, J. Frank, J. Chen, Scalar profiles and NO formation in laminar opposed-flow partially premixed methane/air flames, Combustion and Flame 127 (3) (2001) 2102–2118, elsevier.
- [17] B. Leckner, Spectral and total emissivity of water vapor and carbon dioxide, Combustion and Flame 19 (1972) 33–48.
- [18] D. Goodwin, An open source, extensible software suite for CVD process simulation, California Institute of Technology, Division of Engineering and Applied Science (2003).
- [19] G. Smith, D. Golden, M. Frenklach, N. Moriarty, B. Eiteneer, M. Goldenberg, C. Bowman, R. Hanson, S. Song, W. Gardiner, V. Lissianski, Z. Qin, GRI-Mech 3.0, [http://www.me.berkeley.edu/gri\\_mech/](http://www.me.berkeley.edu/gri_mech/) (2000).
- [20] A. Konnov, Development and validation of a detailed reaction mechanism for the combustion of small hydrocarbons, Twenty-Eighth Symposium (International) on Combustion (2000) 317.

- [21] J. Warnatz, U. Maas, R. Dibble., Combustion - physical and chemical fundamentals, modeling and simulation, experiments, pollutant formation, 4th Edition, Springer Berlin Heidelberg New York, 2006.
- [22] F. Joos, Technische Verbrennung, Springer, 2006, iISBN 10-3-540-34333-4.